Atmos. Chem. Phys. Discuss., 14, 21037–21063, 2014
www.atmos-chem-phys-discuss.net/14/21037/2014/
doi:10.5194/acpd-14-21037-2014

Atmospheric Chemistry and Physics Discussions

An estimation of the $^{18}O/^{16}O$ ratio of UT/LMS ozone based on artefact CO in air sampled during CARIBIC flights

S. Gromov[1] and C. A. M. Brenninkmeijer[1]

[1]Max Planck Institute for Chemistry, Mainz, Germany

Received: 25 July 2014 – Accepted: 6 August 2014 – Published: 15 August 2014

Correspondence to: S. Gromov (sergey.gromov@mpic.de)

Published by Copernicus Publications on behalf of the European Geosciences Union.

Abstract

An issue of ozone-driven artefact production of CO in the UT/LMS air analysed in the CARIBIC-1 project is being discussed. By confronting the CO mixing / isotope ratios obtained from different analytical instrumentation, we (1) reject natural/artificial sampling and mixing effects as possible culprits of the problem, (2) ascertain the photochemical nature and quantify the strength of the effect in a general contamination kinetic framework and, (3) demonstrate the successful application of the isotope mass-balance calculations for inferring the isotope signature of the contamination source. The $^{18}O/^{16}O$ ratios of the latter unambiguously indicate the oxygen being inherited from ozone. The $^{13}C/^{12}C$ ratios hint at reactions of trace amounts of organics with ample stratospheric O_3 that could have yielded the artificial CO. While the exact contamination mechanism is not known, it is clear that the issue pertains only to the earlier (first) phase of the CARIBIC project. Finally, estimated UT/LMS ozone $^{18}O/^{16}O$ ratios are lower than those observed in the LMS within the same temperature range, suggesting that higher pressures (240–270 hPa) inhibit isotope fractionation controlling the local $\delta^{18}O(O_3)$ value.

1 Introduction

Successful determination of the atmospheric carbon monoxide (CO) content based on the collection of air samples depends on the preservation of the mixing ratio of CO inside the receptacle, from the point of sampling to the moment of physiochemical analysis in a laboratory. A famous example is the filling of pairs of glass flasks at South Pole Station for the much later analysis at NOAA in Boulder, Colorado, USA (Novelli et al.,1998). Such was not the case for the study presented here: for air collected in stainless steel tanks in the upper troposphere/lowermost stratosphere (UT/LMS) we observed higher CO values than measured concomitantly in-situ. Moreover, measurement of the stable oxygen isotopic composition of CO from these tanks indicated

ACPD
14, 21037–21063, 2014

additional isotopic enrichments in ^{18}O of 10‰ and greater. It was soon realised that this phenomenon was due to the formation of CO in these tanks and/or in the sampling system and inlet tubing used, by reactions involving ozone (Brenninkmeijer et al., 1999).

Unexpectedly high $^{18}O/^{16}O$ ratios in stratospheric ozone (O_3) were discovered by Konrad Mauersberger using a balloon-borne mass spectrometer (Mauersberger, 1981). The causes for the atypical ^{18}O and the subsequently discovered concomitant disproportionately high ^{17}O enrichments of stratospheric O_3 were subject to a series of studies of theoretical and experimental nature (see, e.g., Schinke et al. (2006) for a review). However, measurement of the isotopic composition of ozone is generally problematic. In the stratosphere its concentrations may be higher, but the remoteness of the sampling domain is a problem. In the troposphere, low O_3 concentrations are the main obstacle, as indicated by few experiments performed to date (Krankowsky et al., 1995; Johnstonand Thiemens, 1997; Vicarsand Savarino, 2014). The recent indirect method of reacting atmospheric ozone with a substrate that can be analysed for the isotopic composition of the O_3-derived oxygen helps a good deal to obtain information on the O_3 isotopic composition (Vicars et al., 2012).

The air samples we refer to here were collected onboard a passenger aircraft carrying an airfreight container with analytical and air/aerosol sampling equipment on long distance passenger flights between Germany and South India/the Caribbean within the framework of the CARIBIC project (Civil Aircraft for the Regular Investigation of the atmosphere Based on an Instrument Container, http://www.caribic-atmospheric.com). Although the increase of CO concentrations in air stored in vessels is a well recognised problem, to our knowledge a specific ozone-related process has not been reported yet. Here we discuss this phenomenon and turn its disadvantageous effect into the advantage of receiving a valid estimate of the oxygen isotopic composition of ozone in the UT/LMS.

ACPD
14, 21037–21063, 2014

2 Experimental

CARIBIC Phase #1 (abbreviated hereafter "C1") was operational from November 1998 until April 2002 using a *Boeing* 767–300 ER operated by LTU International Airlines (Brenninkmeijer et al., 1999). Here, twelve air samples were collected per flight (of ~10 h duration) in stainless steel tanks for analysing the abundance of ^{14}CO. For this purpose, large air samples are required in view of the ultra-low abundance of this mainly cosmogenic tracer (10–100 molecules cm^{-3} STP, about 40–400 amol mol^{-1}). As we mention above, the oxygen isotopic composition of the CO present in these samples was corrupted when ozone levels were high, namely 100–600 nmol mol^{-1} at cruise altitudes of 10–12 km.

CARIBIC Phase #2 (referred to as "C2") started operation in December 2004 with a Lufthansa *Airbus* A340–600 fitted with a new inlet system and air sampling lines, including PFA lined tubing for trace gas intake (Brenninkmeijer et al., 2007). No flask CO mixing / isotope ratio measurement is performed in C2. Nonetheless, when comparing the CO abundances in relation to O_3 mixing ratios for C1 and C2, differences are apparent in the LMS, where C2 CO values are systematically lower. Because the CO levels cannot have changed over the period in question by the difference we find (up to 55 %), artefacts and calibration issues need to be scrutinised.

In addition to the whole air sample (WAS) collection systems, both C1 and C2 measurement setups include different instrumentation for on-line detection of [CO] and [O_3] (hereinafter the squared brackets [] denote the abundance, i.e. concentration or mixing ratio, of the respective species). Thus, the in-situ CO analysis in C2 is done using a vacuum ultraviolet fluorescence (VUV) instrument with lower measurement uncertainty and higher temporal resolution of ± 2 nmol mol^{-1} in ~2 s versus ± 3 nmol mol^{-1} each 130 s in C1 using a gas chromatography (GC)-reducing gas analyser (Zahn et al., 2000; Scharffe et al., 2012). In C2, no analyses of CO from whole air samples were made, in contrast to C1. Furthermore, the detection frequency for ozone mixing ratios has also increased, viz. from 0.06 Hz in C1 to 5 Hz in C2 (Zahn et al.,

ACPD
14, 21037–21063, 2014

2002; Zahn et al., 2012). The C1 WAS samples for the laboratory analyses were collected in stainless steel tanks (holding ∼350 L of air STP) sampled within ∼20 min intervals representing the integral of the compositions encountered along flight segments of ∼250 km. The overall uncertainty of the measured WAS [CO] is less than ±1 % for the mixing ratio and ±0.1 ‰/±0.2 ‰ for $\delta^{13}C(CO)/\delta^{18}O(CO)$, respectively (Brenninkmeijer, 1993; Brenninkmeijer et al., 2001). The isotope compositions are reported throughout this manuscript using $\delta^i = ({}^iR/{}^iR_{st} - 1)$ relating the ratio of rare over abundant isotopes ${}^iR$ of interest (i denotes ^{13}C, ^{18}O or ^{17}O) to the standard ratio ${}^iR_{st}$. These are V-SMOW of 2005.20×10^{-6} for $^{18}O/^{16}O$ (Gonfiantini, 1978; Coplen, 1994) and 386.72×10^{-6} for $^{17}O/^{16}O$ (Assonovand Brenninkmeijer, 2003), and V-PDB of 11237.2×10^{-6} for $^{13}C/^{12}C$ (Craig, 1957), respectively.

Figure 1 presents the LMS CO–O_3 distribution of the C2 measurements overlaid with the C1 in-situ and WAS data. For the in-situ CO datasets we calculated the statistics of the samples with respective O_3 abundances clustered in 20 nmol mol^{-1} bins, i.e. the median and spread (the interquartile range, IQR, is used in the current analysis as a robust measure of the data spread instead of the standard deviation) of [CO] as a function of [O_3] analysed. The data (for C2, until June 2013) exhibit large [CO] variations at [O_3] below 400 nmol mol^{-1} that primarily reflect pronounced seasonal variations in the NH tropospheric CO abundance. With O_3 rising, [CO] increasingly becomes stratospheric, and its spread reduces to mere 3.5 nmol mol^{-1} and less, as [O_3] surpasses 500 nmol mol^{-1}. Despite the comparable spread in C1 and C2 [CO], from 400 nmol mol^{-1} of [O_3] onwards the C1 CO mixing ratios start to level off, with no samples below 35 nmol mol^{-1} having been detected, whereas the C2 levels continuously decline. By the 580 nmol mol^{-1} O_3 bin, C1 [CO] of $39.7^{+0.7}_{-1.3}$ nmol mol^{-1} accommodates some extra 15 nmol mol^{-1} compared to $25.6^{+1.2}_{-1.1}$ nmol mol^{-1} typical for C2 values. Overall, at [O_3] above 400 nmol mol^{-1} the conspicuously high [CO] is marked in about 200 in-situ C1 samples, of which 158 and 69 emerge as statistically significant mild and extreme outliers, respectively, when compared against the ample ($n \sim 3\times10^5$) C2 statis-

ACPD
14, 21037–21063, 2014

tics (the conventions here follow Natrella (2003), i.e. ±1.5 and ±3 IQR ranges define the inner and outer fences of the C2 [CO] distribution in every ozone bin, respectively; the numbers quoted are the sums for the C1 in-situ CO falling in bins with average [O_3] of 420–620 nmol mol^{-1}). None of C1 CO at [O_3] above 560 nmol mol^{-1} agrees with the C2 observations.

Besides the mixing ratios, unnatural elevations in the $^{18}O/^{16}O$ ratios of CO from the WAS measurements are also evident, as shown in Fig. 2. The large $\delta^{18}O(CO)$ departures that reach beyond +16 ‰ are found to be proportional to the concomitant O_3 abundances (denoted with colour) and more prominent at lower [CO]. A rather different relationship, however, is expected from our knowledge of UT/LMS CO sources (plus their isotope signatures) and available in-situ observations (ibid., shown with triangles), as elucidated by Brenninkmeijer et al. (1996) (hereafter denoted as "B96"). That is, the more stratospheric CO is, the greater fraction of its local inventory is refilled with the photochemical component stemming from methane oxidation with a characteristic $\delta^{18}O$ signature of ∼ 0 ‰ or lower (Brenninkmeijerand Röckmann, 1997). This occurs because the CO sink at ruling UT/LMS temperatures proceeds more readily than its production, as the reaction of hydroxyl radical (OH) with CO, being primarily pressure-dependent, outcompetes the temperature-sensitive reaction of OH with CH_4. Furthermore, as the lifetime of CO quickly decreases with altitude, transport-mixing effects take the lead in determining the vertical distributions of [CO] and $\delta^{18}O(CO)$ above the tropopause, i.e. their mutual relationship. This is seen from the B96 data at [CO] below 50 nmol mol^{-1} that line-up in a near linear relationship towards the end-members with lowest $^{18}O/^{16}O$ ratios. The latter equate the largest share of the photochemical component and depletion caused by the CO sink fractionation of ∼ 11 ‰.

It is beyond doubt that the enhancements of C1 $C^{18}O$ originate from ozone, whose large enrichment in heavy oxygen (above +60 ‰ in $\delta^{18}O$, Brenninkmeijer et al., 2003) is unique. In Fig. 2 it is also notable that not only the LMS compositions are affected, i.e. elevations of (3–10) ‰ from the bulk $\delta^{18}O(CO)$ values are present in samples with [CO] of up to ∼ 100 nmol mol^{-1}. These result from the dilution of the least affected tro-

ACPD
14, 21037–21063, 2014

pospheric air with high mixing ratios by CO-poor, however substantially contaminated, stratospheric air, sampled into the same WAS tank. Such sampling-induced mixing renders an unambiguous determination of the artefact source' isotope signature rather difficult, because neither mixing nor isotope ratios of the admixed air portions are known sufficiently well (see below).

Differences between the WAS and in-situ measured [CO] – a possible indication that the $\delta^{18}O(CO)$ contamination pertains specifically to the WAS data – average at $\overline{\Delta}_{WAS-in\text{-}situ} = 5.3 \pm 0.2\,nmol\,mol^{-1}$ (1 SD of the mean, $n = 408$) and happen to be random with respect to any operational parameter or measured characteristic in C1, i.e. irrespective of CO or O_3 abundances. The quoted mixing ratio discrepancy remained after several calibrations between the two systems had been performed, and likely results from the differences in the detection methods, drifts of the calibration standards used (see details in Brenninkmeijer et al., 2001) and a short-term production of CO in the stainless steel tanks during sampling. The large spread of $\Delta_{WAS-in\text{-}situ}$ of $\pm 3.5\,nmol\,mol^{-1}$ (1σ of the population) ensues from the fact that the in-situ sampled air corresponds to (2–4) % of the concomitantly sampled WAS volume, as typically 6–7 in-situ collections of ~ 5 s were made throughout one tank collection of 17–21 min. The integrity of the WAS CO is further affirmed by the unsystematic distribution of the artefact compositions among tanks (an opposite case for $\delta^{18}O(CO_2)$ in C1 is discussed by Assonov et al., 2009). Overall, the WAS and in-situ measured CO mixing ratios correlate extremely well (adj. $R^2 = 0.972$, slope of 0.992 ± 0.008 (1σ), $n = 408$). However, both anomalies in [CO] and $\delta^{18}O(CO)$ manifest clear but complex functions of the concomitant [O_3]. That is, the C1 in-situ and WAS data very likely evidence artefacts pertaining to the ozone-driven effect of the same nature. Below we ascertain and quantify these.

ACPD
14, 21037–21063, 2014

3 Discussion

Three factors may lead to the (artefact) distributions such as seen for C1 in-situ [CO] at the LMS ozone abundances, namely:

1. Strong (linear) natural mixing, such as enhanced stratosphere-troposphere exchange (STE), when a [CO] outside the statistically expected range results from the integration of air having dissimilar ratios of the tracers' abundances, viz. $\rho_{O_3:CO} = [O_3]/[CO]$. For example, mixing of two air parcels in a 15 % : 85 % proportion (by moles of air) with typical $\rho_{O_3:CO}$ of 700 : 24 (stratospheric) and 60 : 125 (tropospheric), respectively, yields an integrated composition with $\rho_{O_3:CO}$ of ∼ 580 : 40 which indeed corresponds to C1 data (this case is exemplified by the mixing curve in Fig. 1). Nonetheless, occurrences of rather high (compared to the typical 24–26 nmol mol^{-1}) stratospheric CO mixing ratios (in our case, ∼ 40 nmol mol^{-1} at the concomitant $[O_3]$ of 500–600 nmol mol^{-1}) are rare. For instance, a deep STE similar to that described by Pan et al. (2004) was observed by C2 only once (cf. the outliers at $[O_3]$ of 500 nmol mol^{-1} in Fig. 1), whereas the C1 outliers were exclusively registered in some 12 flights during 1997–2001. No relation between these outliers and the large-scale [CO] perturbation due to extensive biomass burning in 1997 / 1998 (Novelli et al., 2003) is established, otherwise elevated CO mixing ratios should manifest themselves at lower $[O_3]$ as well. Other tracers detected in CARIBIC provide supporting evidence against such strongly STE-mixed air having been captured by C1. That is, the binned distributions for the water vapour and de-trended N_2O (similar to that for [CO] vs. $[O_3]$ presented in Fig. 1, not shown here) are greatly similar in C1 and C2. Whereas the small relative variations in atmospheric $[N_2O]$ merely confirm matching $[O_3]$ statistics in CARIBIC, the stratospheric $[H_2O]$ distributions witness no $\rho_{O_3:H_2O}$ values corresponding to the C1 outliers' $\rho_{O_3:CO}$, suggesting the latter being unnaturally low.

2. Mixing effects can also occur artificially, originating from sampling peculiarities or data processing. Since the CARIBIC platform is not stationary, about 5 s long sam-

ACPD
14, 21037–21063, 2014

pling of an in-situ air probe in C1 implies integration of the compositions encountered along some hundred metres, owing to the high aircraft speed. This distance may cover a transect between tropospheric and stratospheric filaments of much different compositions. The effect of such "translational mixing" can be simulated by averaging the sampling data with higher temporal frequency over longer time intervals. In this respect, the substantially more frequent CO data in C2 (< 1 s) were artificially averaged over a set of increasing intervals to reckon whether the long sampling period in C1 could be the culprit for skewing its CO–O_3 distribution. As a result, the original C2 data and their averages (equivalent to the C1 CO sample injection time) differ negligibly, as do the respective $\rho_{O_3:CO}$ values; the actual C2 CO–O_3 statistic in the region of interest ([O_3] of 540–620 nmol mol^{-1}) remains insensitive to integration of up to 300 s. Furthermore, a very strong artificial mixing with an averaging interval of at least 1200 s (comparable to C1 WAS sampling time) is required to yield the C2 averages with $\rho_{O_3:CO}$ characteristic for the C1 outliers.

3. In view of the above, it is unlikely that any natural or artificial mixing processes are involved in the stratospheric [CO] discrepancies seen in C1. It therefore stands to reason to conclude that the sample contamination in C1 occurred prior the probed air reaching the analytical/sampling instrumentation in the container, since clearly elevated stratospheric CO mixing ratios are common to WAS and in-situ data. Two more indications, viz. growing [CO] discrepancy with increasing O_3 abundance, and the strong concomitant signal in $\delta^{18}O$ (CO), imply that ozone-mediated photochemical production of CO took place. By confronting the C1 and C2 [CO] measurements in a kinetic framework (detailed in Appendix A), we quantify the artefact CO component varying within 8–18 nmol mol^{-1} throughout the respective [O_3] range of 400–620 nmol mol^{-1}. Subtracting this artefact signal yields the corrected C1 CO–O_3 distribution conformable to that of C2 (cf. red symbols in Fig. 1).

ACPD
14, 21037–21063, 2014

Importantly, we discover the contamination signal being chiefly a function of O_3 abundance only. This allows using the in-situ continuous [O_3] data to estimate the artefact CO in the WAS samples, specifically the isotope ratios of contaminating O_3 and initial CO. As it was mentioned above, the WAS compositions are subject to strong sample-mixing effects which yield obvious $\delta^{18}O(CO)$ outliers even at relatively high [CO] up to 100 nmol mol^{-1}. It is thus necessary to distinguish the proportions and of the least modified (tropospheric) and significantly affected (stratospheric) components, in order to properly correct the composition of the resultant WAS sample mix. On the other hand, the correction approach should be capable of determining the contamination source (i.e., ozone) isotope signature as well.

3.1 Contamination isotope signatures

Practically we resort to the differential mixing model approach (MMA, originally known as the "Keeling-plot"), because it requires only the estimate of the artefact component mixing ratio, but no assumptions on the (unknown) shares and isotope signatures of the air portions mixed in a given WAS tank. The MMA parameterises the admixing of the portion of artefact CO to the WAS sample with the "true" initial composition, as formulated below:

$$\begin{cases} {}^{i}\delta_a C_a = C_t {}^{i}\delta_t + C_c {}^{i}\delta_c \\ C_t \equiv (C_a - C_c) \end{cases},$$

where indices "a", "c" and "t" distinguish the abundances C and isotope compositions ${}^{i}\delta$ (i may refer to ^{13}C or ^{18}O) pertaining to the **a**nalysed sample, estimated **c**ontamination and "**t**rue" composition sought (i.e., C_t and ${}^{i}\delta_t$), respectively. By rewriting the above equation w.r.t. the isotope signature of the admixed portion ${}^{i}\delta_c$, one obtains:

$${}^{i}\delta_c = {}^{i}\delta_t + \left({}^{i}\delta_a - {}^{i}\delta_t\right)\left(1 + C_t/C_c\right), \quad (1)$$

ACPD
14, 21037–21063, 2014

which signifies that linear regression of the measured ${}^{i}\delta_a$ as a function of the reciprocal of C_c yields the estimated contamination signature ${}^{i}\delta_c$ at $(C_c)^{-1} \rightarrow 0$. The MMA described by Eq. (1) provides adequate results only for the invariable initial compositions (C_t, ${}^{i}\delta_t$), therefore we apply it to the subsets of samples picked according to the same reckoned C_t (within a $\pm 2\,\mathrm{nmol\,mol^{-1}}$ window, $n > 7$). Such selection, however, may be insufficient: Due to the strong sampling effects in the WAS samples (see previous section), it is possible to encounter samples that integrate different air masses to the same C_t but rather different average ${}^{i}\delta_t$. The solution in this case is to refer to the goodness of the MMA regression fit, because the R^2 intrinsically measures the linearity of the regressed data, i.e. closeness of the "true" values in a regarded subset of samples, irrespective of underlying reasons for that.

Higher R^2 values thus imply higher consistency of the estimate, as demonstrated in Fig. 3 showing the calculated ${}^{i}\delta_c$ for C_t below $80\,\mathrm{nmol\,mol^{-1}}$ as a function of the regression R^2. The latter decreases with greater C_t (i.e., larger sample subset size, since tropospheric air is more often encountered) and, conformably, larger variations in ${}^{i}\delta_t$. Ultimately, at lower R^2 the inferred ^{18}O signatures converge to values slightly above zero expected for uncorrelated data, i.e. C1 $\delta^{18}O(CO)$ tropospheric average. A similar relationship is seen for the ^{13}C signatures (they converge around $-28\,‰$), however, there are no consistent estimates found (R^2 is generally below 0.4). Since such is not the case for $\delta^{18}O$, the MMA is not sufficiently sensitive to the changes caused by the contamination, which implies that the artefact CO $\delta^{13}C$ should be within the range of the "true" $\delta^{13}C(CO)$ values. Interestingly, the MMA is rather responsive to the growing fraction of the CH_4-derived component in CO with increasing $[O_3]$, as the ${}^{13}C\delta_c$ value of $-(47.2 \pm 5.8)\,‰$ inferred at R^2 above 0.4 is characteristic for the $\delta^{13}C$ of methane in the UT/LMS. It is noteworthy that we have accounted for the biases in the analysed C1 WAS $\delta^{13}C(CO)$ expected from the mass-independent isotope composition of ozone (see details in Appendix B).

ACPD
14, 21037–21063, 2014

We derive the "best-guess" estimate of the admixed CO ^{18}O signature at $^{18}O\delta_c = +(92.0 \pm 8.3)$‰, which agrees with other estimates at R^2 above 0.75. Taking the same subsets of samples, the concomitant ^{13}C signature matches $^{13}C\delta_c = -(23.3 \pm 8.6)$‰, indeed at the upper end of the expected LMS δ^{13}C(CO) variations of −(25–31)‰, which likely does not allow the MMA to ascertain this result as pertaining to the contamination (the corresponding R^2 values are below 0.1). Upon the correction using the inferred $^{18}O\delta_c$ value, the C1 WAS δ^{18}O(CO) data appear adequate (shown with red symbols in Fig. 2). That is, variations in the observed C^{18}O are driven by (1) the seasonal/changes in the composition of tropospheric air and by (2) the degree of mixing or substitution of the latter with the less variable in ^{18}O stratospheric component. This is seen as stretching of the scattered tropospheric values ([CO] above 60 nmol mol^{-1}) in a mixing fashion towards δ^{18}O(CO) of around −10‰ at [CO] of ∼25 nmol mol^{-1}, respectively. The corrected C1 δ^{13}C(CO) data (not shown here) are found to be in a ±1‰ agreement with the observations by B96, except for the deep stratospheric samples ([CO] below 30 nmol mol^{-1}). The latter were encountered in the ozone hole conditions and carried extremely low ^{13}CO abundances, which was attributed to the reaction of methane with available free Cl radicals (Brenninkmeijer et al., 1996).

At last, the plausibility of the obtained results should be verified through the initial values singled out by the MMA, i.e. that the artefact CO was not admixed into the samples with unrealistic "true" compositions. The estimates presented here are based on $C_t = 69 \pm 1$ nmol mol^{-1}, $^{18}O\delta_t = -(2.5 \pm 0.7)$‰ and $^{13}C\delta_t = -(29.0 \pm 1.2)$‰ ($1\sigma$), which are compatible with the B96 observations as well.

3.2 Estimate of $\delta^{18}O(O_3)$

The $^{18}O\delta_c$ signature inferred here unambiguously pertains to ozone and is comparable to the $\delta^{18}O(O_3)$ measured in the LMS at temperatures about 30 K lower than those encountered in C1 (see Table 1 for comparison). If no other factors are involved (see

ACPD
14, 21037–21063, 2014

below), this discrepancy in $\delta^{18}O(O_3)$ should be attributed to the local conditions, i.e. the higher pressures (typically 240–270 hPa for C1 cruising altitudes) at which ozone was formed. Indeed, the molecular lifetime (the period through which the species' isotope reservoir becomes entirely renewed, as opposed to the "bulk" lifetime) of O_3 encountered along the C1 flight routes is estimated on the order of minutes to hours at daylight (H. Riede, MPI-C, 2010), thus the isotope composition of the photochemically regenerated O_3 resets quickly according to the local conditions. Virtual absence of sinks, in turn, leads to "freezing" of the $\delta^{18}O(O_3)$ value during night in the UT/LMS. Verifying the current $\delta^{18}O(O_3)$ estimate against the kinetic data, in contrast to the LMS case, is problematic. The laboratory studies on ozone formation to date have scrutinised the concomitant kinetic isotope effects (KIEs) as a function of temperature at only low pressures (50 Torr); the attenuation of the KIEs with increasing pressure was studied only at room temperatures (see Table 1, also Brenninkmeijer et al. (2003) for references). A rather crude attempt may be undertaken by conjecturing an inhibition of the formation KIEs proportional to that measured at ∼320 K, however applied to the nominal low-pressure values reckoned at (220–230) K. A decrease in $\delta^{18}O(O_3)$ of about (5.9–7.6) ‰ is expected from such calculation, yet accounting for a mere one-half of the (13.3–14.6) ‰ "missing" in $^{18}O\delta_c$.

Lower $^{18}O\delta_c$ values could result from possible isotope fractionation accompanying the production of the artefact CO. Although not quantifiable here, oxygen KIEs in the $O_3 \rightarrow CO$ conversion chain cannot be ruled out, recalling that the intermediate reaction steps are not identifiable and the artefact CO represents at most 4 % of all ozone molecules. Furthermore, the yield λ_{O3} of CO from O_3 may be lower than unity (see details in Appendix A). On the other hand, the inference that the artefact source strength primarily depends on $[O_3]$ corroborates that all secondary O available from O_3 becomes converted to CO, i.e. fractionation effects here should be minimal. In this respect, the unknown ^{13}C KIEs may play a more substantial (than the ^{18}O KIEs) role in determining the $^{13}C\delta_c$ value, owing to the readily available C for the artefact CO production.

ACPD
14, 21037–21063, 2014

Besides KIEs, the selectivity of the ozone atoms transfer to CO may intervene. The terminal O atoms in O_3 are expected to be enriched w.r.t. to the molecular (bulk) ozone composition when the latter is above ~ +70 ‰ in $\delta^{18}O$ (Janssen, 2005; Bhattacharya et al., 2008), therefore an incorporation of only central O into the artefact CO should result in lowering of the ${}^{18}O\delta_c$ value. Such exclusive selection is, however, less likely from the kinetic standpoint and was not observed in available laboratory studies (see Savarino et al. (2008) for a review). For instance, Röckmann et al. (1998a) established the evidence of direct O transfer from ozone to the CO produced in alkene ozonolysis. A reanalysis of their results (in light of findings of Bhattacharya et al., 2008) suggests that usually the terminal O_3 atoms become transferred (their ratio over the central ones changes from the bulk ~ 2 : 1 to ~ 1 : 0 for various species). Considering the alternatives of the O transfer in our case (listed additionally in Table 1), the equiprobable incorporation of the terminal and central ozone atoms into CO should result in the $\delta^{18}O(O_3)$ value in agreement with the "crude" estimate based on laboratory data given above.

Furthermore, the conditions that upheld the reaction of ozone (or its derivatives) followed by the production of CO are vague. A few hypotheses ought to be scrutinised here. First, a fast $O_3 \rightarrow CO$ conversion must have occurred, owing to short (i.e., fraction of a second) exposure time of the probed air to the contamination. Accounting for the typical C1 air sampling conditions (these are: sampled air pressure of 240–270 hPa and temperature of 220–235 K outboard to 275–300 K inboard, sampling rate of $\sim 12.85 \times 10^{-3}$ moles s^{-1} corresponding to 350 L STP sampled in 1200 s, inlet/tubing volume gauged to yield exposure times of 0.01 to 0.1 s due to variable air intake rate, $[O_3]$ of 600 nmol mol^{-1}), the overall reaction rate coefficient (k_c in Eq. (A1) from Appendix A) must be on the order of $6 \times 10^{-15}/\tau_c$ [molec^{-1} cm^3 s^{-1}], where τ_c is the exposure time. Assuming the case of a gas-phase CO production from a recombining ozone derivative and an unknown carbonaceous compound X, the reaction rate coefficient for the latter (${}^{X}k_r$ in Eq. (A1) in Appendix A) must be rather high, at least $\sim 6 \times 10^{-10}$ [molec^{-1} cm^3 s^{-1}] over $\tau_c = 1/100$ s. This number decreases proportionally with growing τ_c and [X], if we take less strict exposure conditions. Nonetheless,

ACPD
14, 21037–21063, 2014

in order to provide the amounts of artefact CO we detect, a minimum abundance of 20 nmol mol^{-1} (or up to 4 µg of C per flight) of X is required, which is not available in the UT/LMS from the species readily undergoing ozonolysis, e.g. alkenes.

Second, a more complex heterogeneous chemistry on the inner surface of the inlet or supplying tubing may be involved. Such can be the tracers' surface adsorption, (catalytic) decomposition of ozone and its reaction with organics or with surface carbon that also may lead to the production of CO (Oyama, 2000). Evidence exists for the dissociative adsorption of O_3 on the surfaces with subsequent production of the reactive atomic oxygen species (see, e.g., Li et al., 1998, also Oyama, 2000). It is probable that sufficient amounts of organics have remained on the walls of the sampling line exposed to highly polluted tropospheric air, to be later broken down by the products of the heterogeneous decomposition of the ample stratospheric O_3. Unfortunately, the scope for a detailed quantification of implex surface effects in the C1 CO contamination problem is very limited.

4 Conclusions

Recapitulating, the in-situ measurements of CO and O_3 allowed us to unambiguously quantify the artefact CO production from ozone likely in the sample line of the CARIBIC-1 instrumentation. Strong evidence to that is provided by the isotope CO measurements. We demonstrate the ability of the simple mixing model approach (e.g., "Keeling-plot") to single out the contamination isotope signatures even in the case of a large sampling-induced mixing of the air with very different compositions. Obtained as a collateral result, the estimate of the $\delta^{18}O(O_3)$ in the UT/LMS appears adequate, calling, however, for additional laboratory data (e.g., the temperature-driven variations of the O_3 formation KIE at pressures above 100 hPa) for a more unambiguous verification.

ACPD
14, 21037–21063, 2014

Appendix A: Contamination kinetic framework

We infer the ozone-exclusive functional dependence of the contamination strength C_c by discriminating the C1 outliers from respective C2 data in the following kinetic framework:

$$O_3 \xrightarrow{^{O_3}k_1} \left(\begin{pmatrix} \ldots + X \xrightarrow{^{X}k_r} \ldots \end{pmatrix}_{K} \atop \begin{pmatrix} \ldots + O_3 \xrightarrow{^{O_3}k_r} \ldots \end{pmatrix}_{(\kappa-1)} \right) \rightarrow \lambda_{O_3} CO\,, \tag{A1}$$

$$C_c = \int_{\tau_c} \prod_{\kappa}{}^{O_3}k_r\,[O_3] \prod_{K}{}^{X}k_r\,[X]\,dt = \lambda_{O_3} k_c\,[O_3]^{\kappa}\,\tau_c$$

where k_c denotes the overall pseudo-first-order rate coefficient of the reaction chain leading to the artefact CO production with the respective yield λ_{O_3}. The individual rate coefficients $^{X}k_r$ and $^{O_3}k_r$ pertain to the unknown compound(s) X and ozone reacting with the integral stoichiometry factors K and κ, respectively. The relation defined by Eq. (A1) provides the best approximation for C_c as a function of $[O_3]$ at $\kappa = 2.06 \pm 0.38$, suggesting two chain steps involving O_3 or its derivatives. At $\kappa = 2$, the ratio $C_c / [O_3]^2$ (essentially proportional to the reaction time τ_c and overall rate coefficient k_c) is found to be $(5.19 \pm 0.12) \times 10^{-5}$ (mol nmol^{-1}) (adj. $R^2 = 0.83$, red. $\chi^2 = 4.0$). The low uncertainty (within ±3 %) of this estimate signifies a mere dependence of the contamination source on the ozone abundance, as well as much comparable reaction times τ_c. It is possible to constrain the overall yield λ_{O_3} of CO molecules in the artefact source chain to be between 0.5 and 1, comparing the magnitude of C_s to the discrepancy between the $[O_3]$ measured in C1 and C2 (±20 nmol mol^{-1}, taken equal to the $[O_3]$ bin size owing to the N_2O–O_3 and H_2O–O_3 distributions matching well between the datasets). Lower λ_{O_3} values, otherwise, should have resulted in a noticeable (i.e., greater than 20 nmol mol^{-1}) decrease in the C1 O_3 abundances with respect to the C2 levels.

ACPD
14, 21037–21063, 2014

Appendix B: Corrections to measured $\delta^{13}C(CO)$ values due to the oxygen MIF

The $\delta^{13}C(CO)$ values went through the ancillary correction owing to the specifics of the laboratory determination of the CO isotopologues' abundances by mass spectrometry. Atmospheric O_3 carries an anomalous composition (or mass-independent fractionation, MIF) with a substantially higher relative enrichment in ^{17}O over that in ^{18}O (above +25 ‰ in $\Delta^{17}O = (\delta^{17}O+1)/(\delta^{18}O+1)^{\beta} - 1$, $\beta = 0.528$) when compared to the majority of terrestrial oxygen reservoirs that are mass-dependently fractionated (i.e., with $\Delta^{17}O$ of ~ 0 ‰) (see Brenninkmeijer et al. (2003) and refs. therein). CO itself also has an unusual oxygen isotopic composition, possessing a moderate tropospheric MIF of around +5 ‰ in $\Delta^{17}O(CO)$ induced by the sink KIEs in reaction of CO with OH (Röckmann et al., 1998b, 2002) and a minor source effect from the ozonolysis of alkenes (Röckmann et al., 1998a; Gromov et al., 2010). A substantial contamination of CO by ozone oxygen induces proportional changes to $\Delta^{17}O(CO)$ that largely exceed its natural atmospheric variation. Furthermore, the MIF has implications in the analytical determination of $\delta^{13}C(CO)$, because the presence of $C^{17}O$ species interferes with the mass-spectrometric measurement of the abundances of ^{13}CO possessing the same basic molecular mass (m/e is 45). When inferring the exact $C^{17}O/C^{18}O$ ratio in the analysed sample is not possible, analytical techniques usually involve assumptions (e.g., mass-dependently fractionated compositions or a certain non-zero $\Delta^{17}O$ value) with respect to the $C^{17}O$ abundances (Assonov and Brenninkmeijer, 2001). In effect for the C1 CO data, the artefact CO produced from O_3 had contributed with unexpectedly high $C^{17}O$ abundances that led to the overestimated $\delta^{13}C(CO)$ analysed. Knowing the contamination magnitude C_c and assuming the typical O_3 MIF composition being $^{17}O\Delta_c$, the respective bias $^{13}C\delta_b$ is calculated using

$$\begin{cases} \Delta^{17}O(CO) \cong \left({}^{17}O\Delta_t C_t + {}^{17}O\Delta_c C_c\right)(C_a)^{-1} \\ {}^{13}C\delta_b = 7.2568 \times 10^{-2}\Delta^{17}O(CO) \end{cases}, \quad \text{(B1)}$$

ACPD
14, 21037–21063, 2014

where $^{17}O\Delta_t$ denotes the natural, i.e. expected "true" value of $\Delta^{17}O(CO)$. The remaining parameters pertain to the contamination kinetic framework (see Appendix A, Eq. A1). For the purpose of the current estimate it is sufficient to take $^{17}\Delta_n$ of +5 ‰ representing equilibrium enrichments expected in the remote free troposphere and UT/LMS. For the ozone MIF signature $^{17}\Delta_c$, the value of +30 ‰ (the average $\Delta^{17}O(O_3)$ expected from the kinetic laboratory data at conditions met along the C1 flight routes, see Sect. 3.2 and Table 1) is adopted. The coefficient that proportionates $^{13}C\delta_b$ and $\Delta^{17}O$ in Eq. (B1) is reckoned for the CO with initially unaccounted MIF (e.g., the sample is assumed to be mass-dependently fractionated) and quantifies some extra +0.73 ‰ in the analysed $\delta^{13}C(CO)$ per every +10 ‰ of $\Delta^{17}O(CO)$ excess (Assonov and Brenninkmeijer, 2001). The most contaminated C1 WAS CO probes at $[O_3]$ above 300 nmol mol^{-1} are estimated to bear $\Delta^{17}O(CO)$ of (6–12) ‰ corresponding to fractions of (0.10–0.27) of the artefact CO in the sample. Accordingly, the reckoned $\delta^{13}C(CO)$ biases span (0.5–0.9) ‰. Although not large, these well exceed the $\delta^{13}C(CO)$ measurement precision of ±0.1 ‰ and were taken into account in the calculations with the MMA presented in Sect. 3.1.

Acknowledgements. The authors are indebted to Claus Koeppel, Dieter Scharffe and Andreas Zahn for their work and expertise on the carbon monoxide and ozone measurements in C1 and C2. Hella Riede is acknowledged for comprehensive estimates of the species lifetimes along the CARIBIC flight routes. We are grateful to Taku Umezawa and Angela K. Baker for the helpful discussions and comments on the manuscript.

The service charges for this open access publication
have been covered by the Max Planck Society.

ACPD
14, 21037–21063, 2014

References

Assonov, S. S. and Brenninkmeijer, C. A. M.: A new method to determine the ^{17}O isotopic abundance in CO_2 using oxygen isotope exchange with a solid oxide, Rapid Commun. Mass Spectrom., 15, 2426–2437, doi:10.1002/rcm.529, 2001.

Assonov, S. S. and Brenninkmeijer, C. A. M.: A redetermination of absolute values for $^{17}R_{VPDB-CO2}$ and $^{17}R_{VSMOW}$, Rapid Commun. Mass Spectrom., 17, 1017–1029, doi:10.1002/Rcm.1011, 2003.

Assonov, S. S., Brenninkmeijer, C. A. M., Koeppel, C., and Röckmann, T.: CO_2 isotope analyses using large air samples collected on intercontinental flights by the CARIBIC Boeing 767, Rapid Commun. Mass Spectrom., 23, 822–830, doi:10.1002/rcm.3946, 2009.

Bhattacharya, S. K., Pandey, A., and Savarino, J.: Determination of intramolecular isotope distribution of ozone by oxidation reaction with silver metal, J. Geophys. Res.-Atmos., 113, D03303, doi:10.1029/2006jd008309, 2008.

Brenninkmeijer, C. A. M.: Measurement of the abundance of ^{14}CO in the atmosphere and the $^{13}C/^{12}C$ and $^{18}O/^{16}O$ ratio of atmospheric CO with applications in New Zealand and Antarctica, J. Geophys. Res.-Atmos., 98, 10595–10614, doi:10.1029/93JD00587, 1993.

Brenninkmeijer, C. A. M., Müller, R., Crutzen, P. J., Lowe, D. C., Manning, M. R., Sparks, R. J., and van Velthoven, P. F. J.: A large ^{13}CO deficit in the lower Antarctic stratosphere due to "Ozone Hole" Chemistry: Part I, Observations, Geophys. Res. Lett., 23, 2125–2128, doi:10.1029/96gl01471, 1996.

Brenninkmeijer, C. A. M. and Röckmann, T.: Principal factors determining the $^{18}O/^{16}O$ ratio of atmospheric CO as derived from observations in the southern hemispheric troposphere and lowermost stratosphere, J. Geophys. Res.-Atmos., 102, 25477–25485, doi:10.1029/97JD02291, 1997.

Brenninkmeijer, C. A. M., Crutzen, P. J., Fischer, H., Gusten, H., Hans, W., Heinrich, G., Heintzenberg, J., Hermann, M., Immelmann, T., Kersting, D., Maiss, M., Nolle, M., Pitscheider, A., Pohlkamp, H., Scharffe, D., Specht, K., and Wiedensohler, A.: CARIBIC – Civil aircraft for global measurement of trace gases and aerosols in the tropopause region, J. Atmos. Oceanic Technol., 16, 1373–1383, doi:10.1175/1520-0426(1999)016<1373:Ccafgm>2.0.Co;2, 1999.

ACPD
14, 21037–21063, 2014

Brenninkmeijer, C. A. M., Koeppel, C., Röckmann, T., Scharffe, D. S., Bräunlich, M., and Gros, V.: Absolute measurement of the abundance of atmospheric carbon monoxide, J. Geophys. Res.-Atmos., 106, 10003–10010, doi:10.1029/2000jd900342, 2001.

Brenninkmeijer, C. A. M., Janssen, C., Kaiser, J., Röckmann, T., Rhee, T. S., and Assonov, S. S.: Isotope effects in the chemistry of atmospheric trace compounds, Chem. Rev., 103, 5125–5161, doi:10.1021/Cr020644k, 2003.

Brenninkmeijer, C. A. M., Crutzen, P., Boumard, F., Dauer, T., Dix, B., Ebinghaus, R., Filippi, D., Fischer, H., Franke, H., Frieß, U., Heintzenberg, J., Helleis, F., Hermann, M., Kock, H. H., Koeppel, C., Lelieveld, J., Leuenberger, M., Martinsson, B. G., Miemczyk, S., Moret, H. P., Nguyen, H. N., Nyfeler, P., Oram, D., O'Sullivan, D., Penkett, S., Platt, U., Pupek, M., Ramonet, M., Randa, B., Reichelt, M., Rhee, T. S., Rohwer, J., Rosenfeld, K., Scharffe, D., Schlager, H., Schumann, U., Slemr, F., Sprung, D., Stock, P., Thaler, R., Valentino, F., van Velthoven, P., Waibel, A., Wandel, A., Waschitschek, K., Wiedensohler, A., Xueref-Remy, I., Zahn, A., Zech, U., and Ziereis, H.: Civil Aircraft for the regular investigation of the atmosphere based on an instrumented container: The new CARIBIC system, Atmos. Chem. Phys., 7, 4953–4976, doi:10.5194/acp-7-4953-2007, 2007.

Coplen, T. B.: Reporting of stable hydrogen, carbon, and oxygen isotopic abundances (Technical Report), Pure Appl. Chem., 66, 273–276, doi:10.1351/pac199466020273, 1994.

Craig, H.: Isotopic standards for carbon and oxygen and correction factors for mass-spectrometric analysis of carbon dioxide, Geochim. Cosmochim. Acta, 12, 133–149, doi:10.1016/0016-7037(57)90024-8, 1957.

Gonfiantini, R.: Standards for Stable Isotope Measurements in Natural Compounds, Nature, 271, 534–536, 1978.

Gromov, S., Jöckel, P., Sander, R., and Brenninkmeijer, C. A. M.: A kinetic chemistry tagging technique and its application to modelling the stable isotopic composition of atmospheric trace gases, Geosci. Model Dev., 3, 337–364, doi:10.5194/gmd-3-337-2010, 2010.

Guenther, J., Erbacher, B., Krankowsky, D., and Mauersberger, K.: Pressure dependence of two relative ozone formation rate coefficients, Chem. Phys. Lett., 306, 209–213, doi:10.1016/S0009-2614(99)00469-8, 1999.

Janssen, C.: Intramolecular isotope distribution in heavy ozone ($^{16}O^{18}O^{16}O$ and $^{16}O^{16}O^{18}O$), J. Geophys. Res.-Atmos., 110, D08308, doi:10.1029/2004jd005479, 2005.

Johnston, J. C. and Thiemens, M. H.: The isotopic composition of tropospheric ozone in three environments, J. Geophys. Res.-Atmos., 102, 25395–25404, doi:10.1029/97jd02075, 1997.

ACPD
14, 21037–21063, 2014

Janssen, C., Guenther, J., Krankowsky, D., and Mauersberger, K.: Temperature dependence of ozone rate coefficients and isotopologue fractionation in ^{16}O-^{18}O oxygen mixtures, Chem. Phys. Lett., 367, 34–38, doi:10.1016/S0009-2614(02)01665-2, 2003.

Krankowsky, D., Bartecki, F., Klees, G. G., Mauersberger, K., Schellenbach, K., and Stehr, J.: Measurement of heavy isotope enrichment in tropospheric ozone, Geophys. Res. Lett., 22, 1713–1716, doi:10.1029/95gl01436, 1995.

Krankowsky, D., Lämmerzahl, P., Mauersberger, K., Janssen, C., Tuzson, B., and Röckmann, T.: Stratospheric ozone isotope fractionations derived from collected samples, J. Geophys. Res.-Atmos., 112, D08301, doi:10.1029/2006jd007855, 2007.

Li, W., Gibbs, G. V., and Oyama, S. T.: Mechanism of Ozone Decomposition on a Manganese Oxide Catalyst. 1. In Situ Raman Spectroscopy and Ab Initio Molecular Orbital Calculations, J. Am. Chem. Soc., 120, 9041–9046, doi:10.1021/ja981441+, 1998.

Mauersberger, K.: Measurement of Heavy Ozone in the Stratosphere, Geophys. Res. Lett., 8, 935–937, doi:10.1029/GI008i008p00935, 1981.

Natrella, M.: NIST/SEMATECH e-Handbook of Statistical Methods, edited by: Croarkin, C. and Tobias, P., NIST/SEMATECH, http://www.itl.nist.gov/div898/handbook/ (last access: 7 May 2014), 2003.

Novelli, P. C., Masarie, K. A., and Lang, P. M.: Distributions and recent changes of carbon monoxide in the lower troposphere, J. Geophys. Res., 103, 19015–19033, doi:10.1029/98jd01366, 1998.

Novelli, P. C., Masarie, K. A., Lang, P. M., Hall, B. D., Myers, R. C., and Elkins, J. W.: Reanalysis of tropospheric CO trends: Effects of the 1997–1998 wildfires, J. Geophys. Res., 108, 4464, doi:10.1029/2002jd003031, 2003.

Oyama, S. T.: Chemical and Catalytic Properties of Ozone, Catal. Rev. Sci. Eng., 42, 279–322, doi:10.1081/cr-100100263, 2000.

Pan, L. L., Randel, W. J., Gary, B. L., Mahoney, M. J., and Hintsa, E. J.: Definitions and sharpness of the extratropical tropopause: A trace gas perspective, J. Geophys. Res.-Atmos., 109, D23103, doi:10.1029/2004jd004982, 2004.

Röckmann, T., Brenninkmeijer, C. A. M., Neeb, P., and Crutzen, P. J.: Ozonolysis of nonmethane hydrocarbons as a source of the observed mass independent oxygen isotope enrichment in tropospheric CO, J. Geophys. Res.-Atmos., 103, 1463–1470, doi:10.1029/97JD02929, 1998a.

ACPD
14, 21037–21063, 2014

Röckmann, T., Brenninkmeijer, C. A. M., Saueressig, G., Bergamaschi, P., Crowley, J. N., Fischer, H., and Crutzen, P. J.: Mass-independent oxygen isotope fractionation in atmospheric CO as a result of the reaction CO+OH, Science, 281, 544–546, doi:10.1126/science.281.5376.544, 1998b.

Röckmann, T., Jöckel, P., Gros, V., Bräunlich, M., Possnert, G., and Brenninkmeijer, C. A. M.: Using ^{14}C, ^{13}C, ^{18}O and ^{17}O isotopic variations to provide insights into the high northern latitude surface CO inventory, Atmos. Chem. Phys., 2, 147–159, doi:10.5194/acp-2-147-2002, 2002.

Savarino, J., Bhattacharya, S. K., Morin, S., Baroni, M., and Doussin, J. F.: The $NO+O_3$ reaction: A triple oxygen isotope perspective on the reaction dynamics and atmospheric implications for the transfer of the ozone isotope anomaly, J. Chem. Phys., 128, 194303, doi:10.1063/1.2917581, 2008.

Scharffe, D., Slemr, F., Brenninkmeijer, C. A. M., and Zahn, A.: Carbon monoxide measurements onboard the CARIBIC passenger aircraft using UV resonance fluorescence, Atmos. Meas. Tech., 5, 1753–1760, doi:10.5194/amt-5-1753-2012, 2012.

Schinke, R., Grebenshchikov, S. Y., Ivanov, M. V., and Fleurat-Lessard, P.: Dynamical Studies Of The Ozone Isotope Effect: A Status Report, Annu. Rev. Phys. Chem., 57, 625–661, doi:10.1146/annurev.physchem.57.032905.104542, 2006.

Vicars, W. C. and Savarino, J.: Quantitative constraints on the ^{17}O-excess ($\Delta^{17}O$) signature of surface ozone: Ambient measurements from 50°N to 50°S using the nitrite-coated filter technique, Geochim. Cosmochim. Acta, 135, 270–287, doi:10.1016/j.gca.2014.03.023, 2014.

Vicars, W. C., Bhattacharya, S. K., Erbland, J., and Savarino, J.: Measurement of the ^{17}O-excess ($\Delta^{17}O$) of tropospheric ozone using a nitrite-coated filter, Rapid Commun. Mass Spectrom., 26, 1219–1231, doi:10.1002/rcm.6218, 2012.

Zahn, A., Brenninkmeijer, C. A. M., Maiss, M., Scharffe, D. H., Crutzen, P. J., Hermann, M., Heintzenberg, J., Wiedensohler, A., Güsten, H., Heinrich, G., Fischer, H., Cuijpers, J. W. M., and van Velthoven, P. F. J.: Identification of extratropical two-way troposphere-stratosphere mixing based on CARIBIC measurements of O_3, CO, and ultrafine particles, J. Geophys. Res., 105, 1527–1535, doi:10.1029/1999jd900759, 2000.

Zahn, A., Brenninkmeijer, C. A. M., Asman, W. A. H., Crutzen, P. J., Heinrich, G., Fischer, H., Cuijpers, J. W. M., and van Velthoven, P. F. J.: Budgets of O_3 and CO in the upper

ACPD
14, 21037–21063, 2014

troposphere: CARIBIC passenger aircraft results 1997–2001, J. Geophys. Res.-Atmos., 107, 4337, doi:10.1029/2001jd001529, 2002.

Zahn, A., Weppner, J., Widmann, H., Schlote-Holubek, K., Burger, B., Kühner, T., and Franke, H.: A fast and precise chemiluminescence ozone detector for eddy flux and airborne application, Atmos. Meas. Tech., 5, 363–375, doi:10.5194/amt-5-363-2012, 2012.

ACPD

14, 21037–21063, 2014

$^{18}O/^{16}O$ ratio of UT/LMS ozone from CARIBIC-1 measurements

S. Gromov and C. A. M. Brenninkmeijer

Table 1. Ozone $^{18}O/^{16}O$ isotope ratios.

Domain	T [K]	P [hPa]	$\delta^{18}O(O_3)$ [‰]	Rem.
LMS	190–210	13–50	83–93 (< 3)	[1]
UT/LMS	220–235	240–270	89–95 (8)	[2]
			84–88 (6)	T
			91–98 (9)	TC
			112–124 (17)	C
Laboratory	190–210	~ 67	87–97 (6)	[3]
	220–235	~ 67	102–110 (6)	[3]
	220–235	240–270	95–103	[4]

Notes: values in parentheses denote the average of the estimates' standard errors. The expected ozone isotope composition on the V-SMOW scale is calculated from the ozone enrichments ε reported relative to O_2 using $\delta^{18}O(O_3)_{V\text{-}SMOW} = \delta^{18}O(O_2)_{V\text{-}SMOW} + {}^{18}O\ \varepsilon(O_3)_{O_2} + [\delta^{18}O(O_2)_{V\text{-}SMOW} \times {}^{18}O\ \varepsilon(O_3)_{O_2}]$.

[1] Observations (see Krankowsky et al. (2007) and refs. therein), lowermost values (19–25 km). Quoted temperature range is derived by matching measured $\delta^{18}O(O_3)$ and laboratory data (see note [3]).

[2] This study, C1 observations (10–12 km). Letters denote the estimates derived using the data from Bhattacharya et al. (2008) and assuming only terminal (T), only central (C) and equiprobable terminal and central (TC) ozone atoms transfer to the artefact CO.

[3] Calculated using the laboratory KIE temperature dependence data summarised by Janssen et al. (2003).

[4] Calculated assuming a pressure dependence of the O_3 formation KIE similar to that measured at 320 K (see Guenther et al. (1999) and refs. therein).

ACPD
14, 21037–21063, 2014

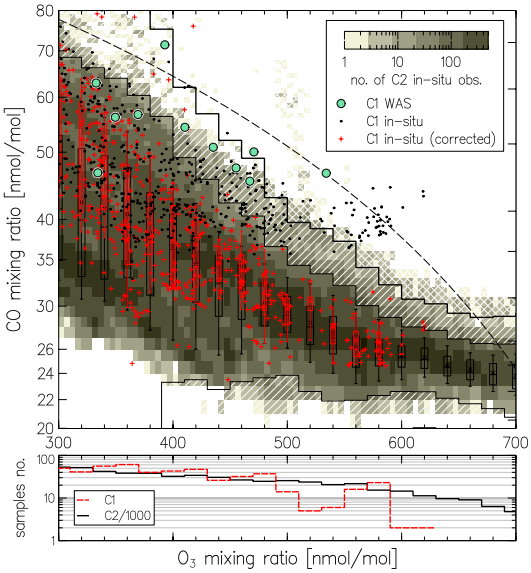

Figure 1. Distribution of CO mixing ratios as a function of concomitant ozone mixing ratios measured by CARIBIC in the LMS ($[O_3] > 300$ nmol mol^{-1}). The shaded area is the two-dimensional histogram of the C2 measurements counted in 5×1 nmol mol^{-1} size $[O_3]$ × [CO] bins, thus darker areas emphasise greater numbers of particular CO–O_3 pairs observed. Small symbols denote the original C1 in-situ measurements (black) and corrected for the artefacts (red); the C1 WAS analyses (11 of total 408) are shown with large symbols. Thin and thick step-lines demark the inner and outer statistical fences of the C2 data clustered in 20 nmol mol^{-1} O_3 bins, respectively; box-and-whisker diagrams present the statistics for the C2 (black) and corrected C1 (red) data (whiskers represent 9th/91st percentiles). The dashed curve exemplifies compositions expected from the linear mixing of very different (e.g., tropospheric and stratospheric) end-members. Lower panel presents the sample statistic for each CARIBIC dataset (note the C2 figures scaled down by a factor of 1000).

ACPD
14, 21037–21063, 2014

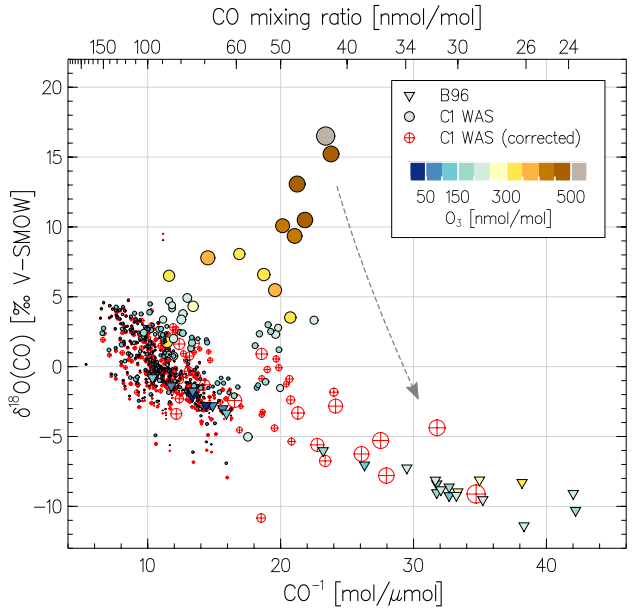

Figure 2. $^{18}O/^{16}O$ isotope composition of CO as a function of its reciprocal mixing ratio. Triangles present the data from the remote SH UT/LMS obtained by Brenninkmeijer et al. (1996) (B96). Colour refers to the concomitantly observed O_3 abundances; note the extremely low $[O_3]$ encountered by B96 in the Antarctic ozone-hole conditions. Filled and hollow circles denote the original and corrected (as exemplified by the dashed arrow) C1 WAS data, respectively, with the symbol size scaling proportional to the estimated contamination magnitude (see text).

ACPD
14, 21037–21063, 2014

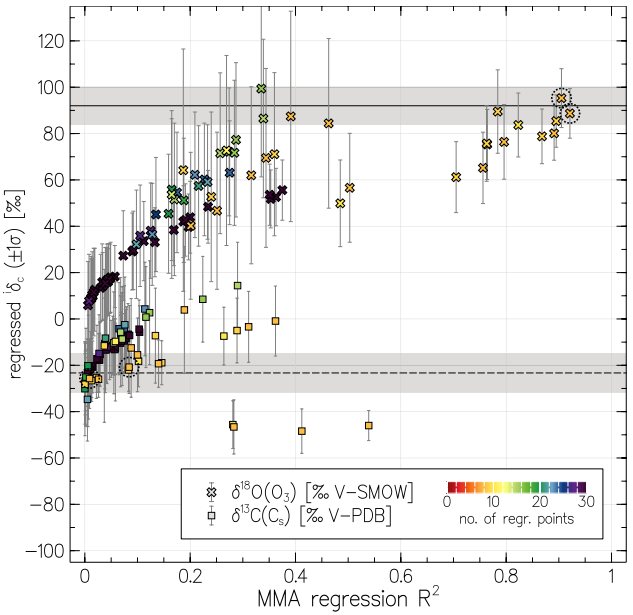

Figure 3. Results of the regression calculation with the MMA. Shown with symbols are the contamination source isotope signatures $^{i}\delta_c$ as a function of the respective coefficient of determination (R^2). Colour denotes the number of samples in each subset selected. Solid and dashed lines present the best guess ±1 SD for the $\delta^{18}O(O_3)$ and $\delta^{13}C(C_c)$ estimates. Dashed circles mark the values obtained at highest R^2 for $^{18}O\delta_t$ regression (above 0.9). See text for details.

ACPD
14, 21037–21063, 2014